Available online at www.sciencedirect.com
ScienceDirect
International Journal of Heat and Mass Transfer 51 (2008) 4427–4438
International Journal of HEAT and MASS TRANSFER
www.elsevier.com/locate/ijhmt

Explosive vaporization and microbubble oscillations on submicron width thin film strip heaters

G. Romera-Guereca, T.Y. Choi [1], D. Poulikakos *

Laboratory of Thermodynamics in Emerging Technologies, Department of Mechanical and Process Engineering, ETH Zurich, CH-8092 Zurich, Switzerland

Received 18 May 2007; received in revised form 6 December 2007
Available online 7 April 2008

Abstract

Boiling induced by an electrically heated submicron strip platinum heater submerged in deionized water is investigated in this work. The temperature evolution of the heater subjected to pulsed heating showed a fast transient behavior followed by a temperature plateau. The boiling initiation temperatures for a host of current intensities were determined and an interesting consistent oscillation in the temperature curve in the plateau region was discovered and analyzed. This oscillation was shown to originate from sequential bubble growth and collapse cycles taking place at a high frequency (MHz). Visualization of the process confirmed the formation of vapor bubbles of ca. 1 μm diameter on the heater.

Keywords: Strip thin film submicron heater; Explosive vaporization; Pulse heating; Temperature oscillation; Bubble oscillation

1. Introduction

Explosive boiling is an abrupt phase change phenomenon taking place in a highly superheated liquid. The liquid can become superheated if it is depressurized rapidly at constant temperature [1] or, as it is the case in the present work, if it is heated rapidly above the saturation temperature while its pressure is maintained constant. Under carefully controlled conditions (no contamination, smooth surfaces and no physical disturbances) it is possible for a liquid to reach a superheated state. Under most practical circumstances, however, the ideal conditions cannot be met and the superheated liquid will return to its equilibrium state through vaporization.

Explosive boiling at the microscale has been used in technology development such as ejection of droplets of ink (ink jet printer) and microfluidic devices actuated by thermally generated bubbles such as drug delivery systems [2], valves [3], pumps [4], fuel injectors [5,6], and microthrusters [7,8]. To realize the potential for commercial applications, a thorough understanding of the involved physical phenomena is needed to better control the process.

Many researchers investigated the physics and controllability of explosive boiling at wires and at thin film heaters [9–13]. Despite the existence of such studies, very little pertains to submicron heaters. The only investigators identified by the present authors are Deng et al. [14] who reported bubble formation on two submicron size heaters. The heater sizes were: 0.5 μm × 0.5 μm and 1 μm × 0.5 μm. In their work, the authors used pulsed heating with a fixed duration of 1.66 ms and the current was adjusted to the minimum required for nucleation within the pulse duration. In these experiments, nucleation took place after a delay of 51–60 μs and at heater temperatures of 245–207 °C, respectively (with corresponding liquid superheat of 145–107 K). The maximum bubble diameter for both heaters was 2.5 ± 0.3 μm. The onset of bubble nucleation was detected by a sudden change in the measured average temperature as a function of time. The achieved heating

* Corresponding author. Tel.: +41 446322738; fax: +41 446321176.
E-mail address: dimos.poulikakos@ethz.ch (D. Poulikakos).
[1] Present address: Department of Mechanical and Energy Engineering, University of North Texas, TX 76203, United States.

0017-9310/$ - see front matter © 2008 Elsevier Ltd. All rights reserved.
doi:10.1016/j.ijheatmasstransfer.2008.01.014

Nomenclature

q''_{l}	heat transfer rate to the fluid	I	electric current
q''_{tl}	total heat transfer rate for the immersed heater	V	voltage drop
q''_{tv}	total heat transfer rate in vacuum	$V_{100\ \Omega}$	voltage drop at the 100 Ω resistor.
R	resistance of the heater element	t	time
R_0	initial resistance of the heater element		
T	heater temperature	*Greek symbols*	
T_0	initial heater temperature	α	temperature coefficient of resistance (K^{-1})
T_b	temperature at boiling incipience	ΔT	heater temperature increase (K)
T_{ps}	pseudo-steady temperature		

rates were of the order of 10^7 K/s with heat transfer rates from the heater of 190.9–112.4 MW/m^2, respectively.

The same group of authors considered the scaling effects of micro bubble actuation [15,16]. Microheaters ranging from 150 μm × 50 μm to 0.5 μm × 0.5 μm were fabricated out of the same wafer to minimize the uncertainties in the measurements induced by fabrication process parameters such as film thickness. Two different vapor region types were observed: 'oblate vapor bubble' for the larger heaters (>10 μm) and 'spherical bubble' for the submicron heaters.

In the present work we present an investigation of explosive boiling on a novel self-sensing heater element. The novelty of this investigation is the small dimension of the heater (<1 μm × 3–6 μm), the device layout which allows for a 4-point, resistive measurement technique, and the physical phenomena sought (bubble formation and behavior and temperature determination at early stages of vaporization). We measured the average temperature increase on a submicron platinum heater subjected to electrical pulses and observed the occurrence of boiling as well as the effect of current intensity at the moment when vaporization is detected. Very high rates of temperature rise were achieved because of the small dimensions of the device, leading to the initiation of vaporization in less than 1 μs.

High frequency temperature oscillations (at MHz) were measured which may be associated with rapid oscillations of the vapor layer thickness taking place on the surface of the heater. Similar oscillatory phenomenon was observed previously in the work by Avedisian et al. [9]; the heater in that case was a 65 μm side square thin film heater such as those used in an HP ink jet printer cartridge. The oscillation appeared at relatively low temperatures and not much attention was dedicated to its physics since the authors focused on the initial explosion leading to a single droplet ejection. The work by Osborne [17] used a metallic wire immersed in a pool of liquid. They measured the sound generated by the boiling phenomena taking place at the wire.

We measured the frequency and amplitude of the temperature oscillations for different current intensities showing that the increase of the current intensity increases the frequency and decreases the amplitude of the temperature oscillations. To the best of our knowledge, this is the first study of the oscillatory phenomenon using thin film resistors.

Visualization of the vapor layer was also achieved using a pulsed image acquisition system synchronized with the heating pulse. Limited temporal resolution of the illumination system did not allow the visualization of the bubble size oscillations but the formation of bubbles of submicron size could be clearly confirmed.

We could not find in the literature other studies where such small diameter bubbles are generated by short electric pulses as herein. In addition, the small size of the heater made possible the generation of an ultrasound source highly concentrated in time and space.

2. Experimental procedures

2.1. Heater fabrication

The substrate of the device was a 300 μm thick silicon wafer. A silicon nitride layer 500 nm thick was grown by using the low-pressure chemical vapor deposition (LPCVD) technique. Chromium (10 nm) and platinum (100 nm) were patterned on this substrate by the standard lift-off technique: First, a layer of photoresist was defined by photolithography. After the deposition of the metal by e-beam evaporation (UNIVEX 550) on top of the exposed substrate (the nitride layer), the photoresist was stripped off in acetone to define the metal patterns.

The entire metal pattern for the 4-wire construction is shown in Fig. 1a. The central region, with a size of a few tenths of a micrometer, was then milled by using a focused ion beam source (FIB). A narrow central region (the heater) could be patterned with the size of half a micron since the ion beam size (typically less than 10 nm) is much smaller than the region of interest. The two small electrodes in the middle were utilized for voltage drop measurement Fig. 1b. A ceramic carrier (28 Lead Side Brazed package, Spectrum,US) was used to interface the micro/nanofabricated chip with the measurement equipment.

2.2. Heater characterization

2.2.1. Submicron heater calibration set-up

The resistor can be used as a temperature sensor because the increase of temperature induces an increase of resis-

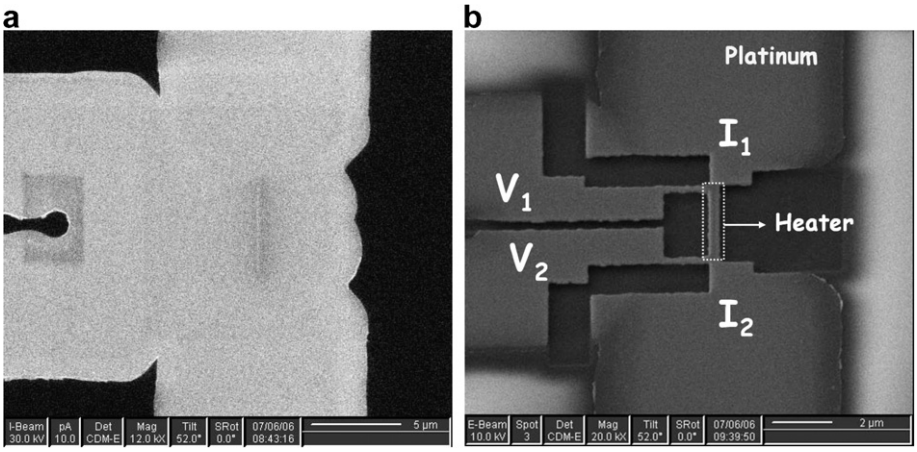

Fig. 1. (a) Metal structure patterned by lift-off before the Focused Ion Beam (FIB) milling. (b) Submicron heater structure (narrow central region enclosed in dashed rectangle) fabricated by milling the initial platinum structure. The voltage drop is measured across the two small electrodes (V_1 and V_2) for localized resistance thermometry.

tance that can be measured with the 4-point arrangement. To obtain the temperature value out of the resistance measurement one needs to measure the temperature coefficient of resistance (α) first. The resistance of the heater element (R) was measured at several heater temperatures (T). The slope of the linear trend of the relative resistance increase, $(R - R_0)/R_0$, to the temperature increase $(T - T_0)$, where R_0 is the initial resistance measured at the initial temperature T_0, provided the α value.

Fig. 2 depicts a sketch of the calibration set-up. It is composed of a metallic vacuum chamber with vacuum pump, a sample holder and the data acquisition unit. The front cover of the chamber has electronic feedthroughs (connectors for electronic supply and measurement), the sample holder being attached. The sample holder has two buried electrical heaters to control the sample temperature. A vacuum pump was connected to the vacuum chamber to minimize the effect of air current on calibration. To monitor the temperature in the sample holder, two temperature sensors (PT100) buried in the holder are connected to the data acquisition unit (HP3852A, Hewlett–Packard).

Uniform heating for minimum temperature gradient in the sample (holder) was ensured by sandwiching the sample between the two aluminum blocks (chip holder) in which the electrical heaters are embedded. The sample is mounted on the ceramic IC packaging chip. The pads in the chip were wirebonded to the microfabricated electrodes nearby

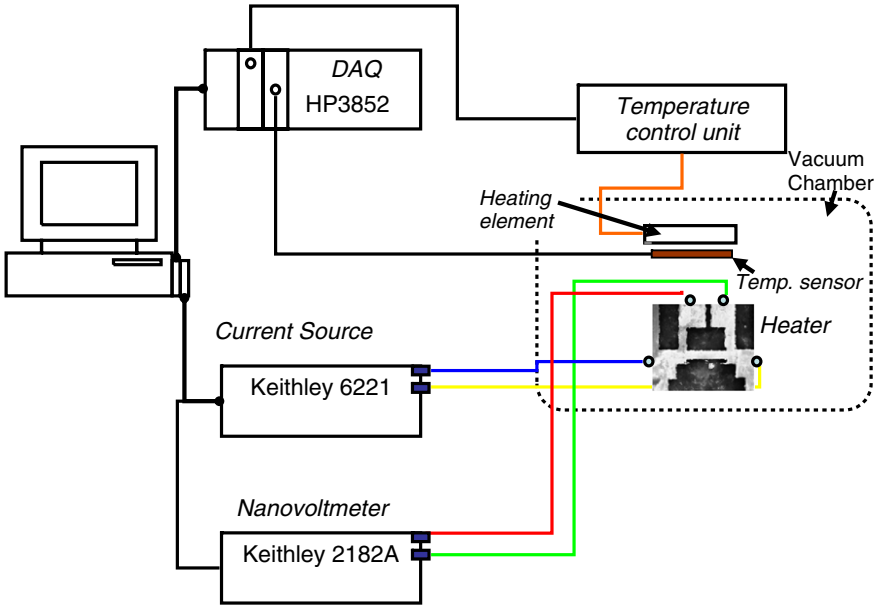

Fig. 2. Heater calibration set-up.

the submicron heater while the leads were fastened to the connectors in the chip holder by metallic screws.

2.2.2. Resistance measurement

For the measurement of resistance during the calibration, a low level current source (model 6221, Keithley) and a Nanovoltmeter (model 2182A, Keithley) were used. The applied current must be kept as small as possible to reduce errors associated with self heating.

Thermoelectric voltages are undesired voltages generated when different parts of a circuit are at different temperatures or when conductors made of dissimilar materials are joined together. When the calibration was performed, a temperature gradient was present in the circuit, especially inside the oven. Because it was not practical to completely avoid the presence of contacts between dissimilar materials and the applied current needed to be small to avoid self heating, the thermoelectric voltages were considerable and needed to be corrected. The thermoelectric voltages were canceled out by using the combination of Keithley 6221 source unit and 2182A Nanovoltmeter. The two instruments were operated in the synchronized-delta mode. Under the delta mode the source unit supplies the current pulses and makes a measurement before and during each pulse. The Keithley 6221 calculates the difference between these two measurements, suppressing any constant thermoelectric offset and displays the true value of the voltage.

2.2.3. I–V characteristics

In order to characterize the heater, the current–voltage characteristic curve (I–V) was determined, showing the relationship between the dc current passing through the submicron heater and the dc voltage across its terminals. Current pulses of 200 μs in duration and of gradually increasing amplitude were supplied to the submicron heater and the corresponding voltage drops were measured. This measurement was performed in vacuum, in air and in water. This characterization curve is useful for two purposes: first, it shows the non-linearity due to the temperature dependence of the resistance and second, because the voltage drop can be converted to temperature, it indicates the amplitude of the current pulse necessary to achieve a desired temperature. According to Ohm's law, for a resistor there is a linear relationship between the applied current and the resulting electrical voltage drop. In our micro/nanofabricated resistor, the applied current increases the temperature of the heater, and an increase of temperature modifies the resistance, therefore the I–V characteristic curve becomes non-linear.

2.3. Experimental set-up for explosive boiling study

2.3.1. Pulsed heating set-up

For the fast heating experiments a pulse generator that has a short settling time (model HP8114A, Hewlett–Packard) was used. It supplied a pulse to a circuit consisting of a 100 Ω resistor connected in series with the submicron heater as shown in Fig. 3. The resistor was used for measuring the current (by measuring the voltage drop across its terminals) and as a voltage divider. A differential amplifier (DA1822A, LeCroy) was connected to the terminals of this resistor. The terminals used to sense the voltage drop across the submicron heater were connected to a second

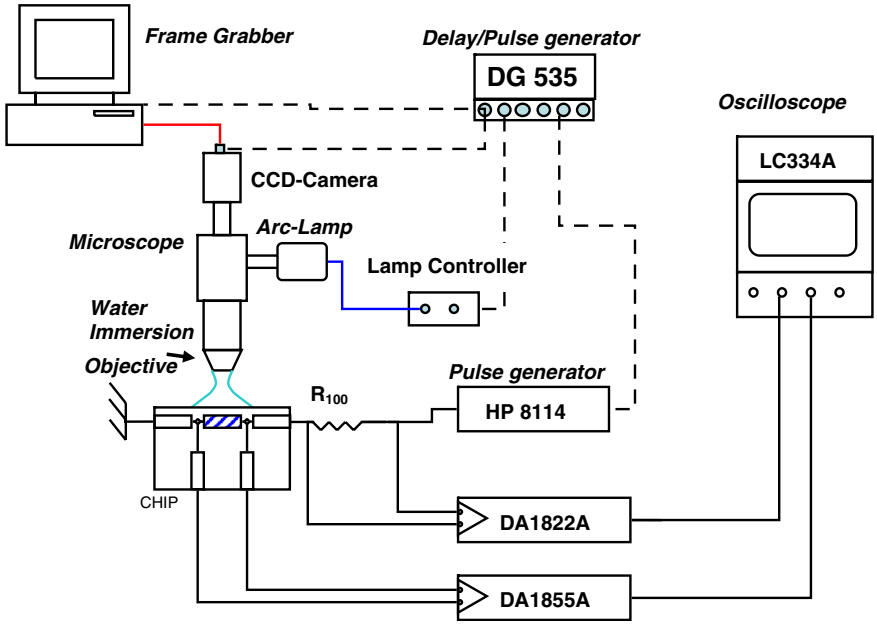

Fig. 3. Set-up for the explosive vaporization experiments and pulsed image acquisition. The 100 Ω resistor is used as a voltage divider. The connections represented with dashed lines are the triggering signals.

differential amplifier (DA1855A, LeCroy). The two signals were monitored with an oscilloscope (LC334A, LeCroy) set to a sampling frequency of 1 GHz. The signals were then exported to a PC via GPIB interface.

The instantaneous current through the circuit at time t was obtained by applying Ohm's law: $I(t) = V_{100\ \Omega}/100\ \Omega$. The instantaneous temperature of the heater (spatially averaged over its surface) can be obtained from the current, $I(t)$ and the voltage drop across the heater, $V(t)$:

$$T(t) = T_0 + \frac{V(t)/I(t) - R_0}{R_0\alpha}. \quad (1)$$

Error analysis. The error in the calculation of the temperature was obtained by determining the partial error induced by each variable appearing in the previous expression 1 and was 6 °C; 2 °C due to the error from measuring the electrical current and the voltage drop across the heater $(I(t), V(t))$, 2 °C due to error associated with the measurement of R_0, 1 °C due to the uncertainty measuring T_0 and less than 1 °C due to the calibration error.

2.3.2. Pulsed image acquisition

The visualization technique is based on flash-lamp illumination on the region of interest at a certain "instance" after triggering the heating process. To achieve this, two pulses with a certain delay between them were generated, triggering first the HP pulse generator and then the flash lamp. The phenomena under investigation could be repeated as long as the time between successive pulses was long enough to return to the initial temperature of the heater. Therefore when the delay between the heating onset and the flash-lamp trigger was kept constant the captured images were always the same, implying a frozen process. If the delay was increased by small increments a series of captured images would signify a slowly moving process.

The image acquisition system was composed of a microscope, (BX60, Olympus, Switzerland), a nanosecond flash light source and its driver, (Nanolite KL-K, High Speed Photo-Systeme, Germany), A CCD camera (CV-M10 Progressive Scan, Stemmer Imaging GmbH, Germany) connected to a frame grabber, (PX-510, Stemmer Imaging GmbH, Germany) as in the system used in [11,18]. The synchronized pulses were generated with a digital delay/pulse generator (DG535, Stanford Research Systems) as in the set-up described in [19]. A schematic diagram of the visualization set-up is depicted in Fig. 3. The dashed lines represent the connections of synchronizing the heating pulse and the visualization system. The visualization was made with a long working-distance, water-immersion objective (LUMPlan FL40xWI, Olympus Schweiz AG) combined with an extra 1.6× magnification, resulting in a total magnification of ×64.

The duration of the flash of light is 100 ns, The jittering of the lamp is about 150 ns, providing a temporal resolution of 250 ns. As it will be seen later, this temporal resolution does not allow to resolve the ultra fast bubble growth process. However, the obtained images clearly confirmed the formation of vapor on the heater.

3. Results and discussion

3.1. Device characterization

3.1.1. Device calibration

Fig. 4 depicts the relationship between the electrical resistance change of the heater and the temperature of the holder for a representative specimen. The electrical resistance of the submicron heater at the corresponding temperature was measured by supplying 4 μA-amplitude current pulses and measuring the induced voltage drop. Using a least-squared fit, the temperature coefficient of resistance $\alpha = ((R - R_0)/R_0)/T - T_0$ was determined to be $1.60 \times 10^{-3} \pm 1 \times 10^{-5}\ \mathrm{K}^{-1}$ ($3.8 \times 10^{-3}\ \mathrm{K}^{-1}$ for bulk platinum).

3.1.2. I–V characteristic and temperature rise for different input powers

Fig. 5a shows the I–V characteristic obtained in vacuum. The solid line represents the characteristic behavior of a resistor equal to the initial resistance of the device. The data points can be used to obtain the values of the resistance $R = V/I$, and the temperature increase can be determined using the expression:

$$\Delta T = \frac{R - R_0}{R_0\alpha}. \quad (2)$$

The volume-averaged temperature rise in the heater as a function of input power ($V \times I$) is shown in Fig. 5b. Because the mass of the heater is very small, the total heat transfer rate from the heater is composed of: (1) conduction to the substrate on which the heater is fabricated; (2) conduction heat transfer to the liquid above the heater; and (3) radiation heat transfer to the surrounding. By neglecting radiation and considering at a given heater temperature the total heat transfer rate in vacuum (q''_{tv}) and the total heat transfer rate when the heater is submerged in

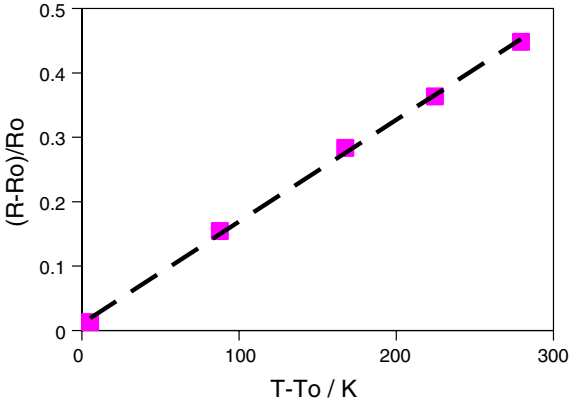

Fig. 4. Measured relative resistance change for different temperatures and linear fit for the calculation of the thermal coefficient of resistance.

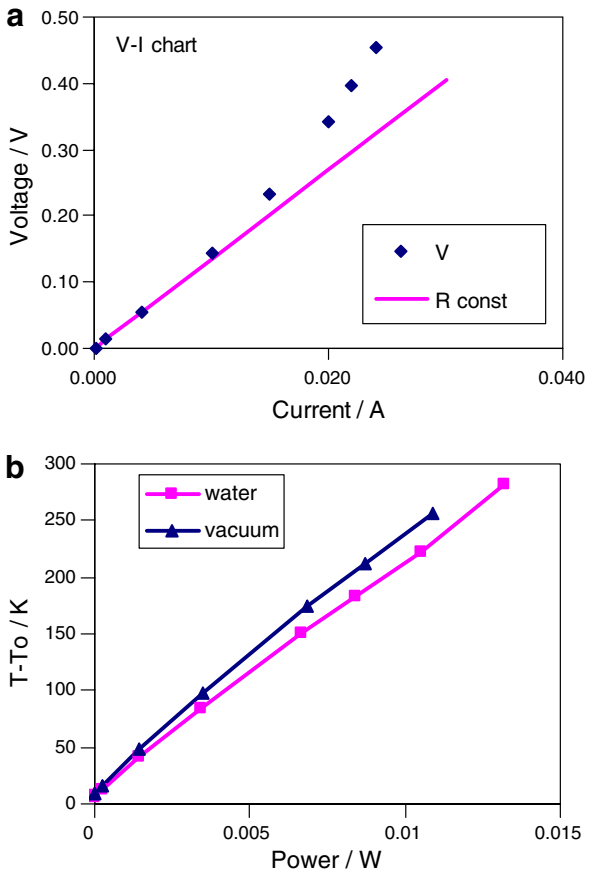

Fig. 5. (a) *V–I* characteristic of a chip of initial $R_0 = 13.60\,\Omega$. The line shows the characteristic of a resistor. (b) Temperature rise versus total power input.

water (q''_{tl}), we can eliminate the need to calculate the heat dissipated to the substrate and write

$$q''_{l} = q''_{tl} - q''_{tv}, \tag{3}$$

where q''_{l} is the heat transfer rate to the fluid. Using the values shown in Fig. 5b the heat transfer rate to the liquid for a temperature of the heater of 250 °C turns out to be 10% of the total electrical power input to the heater. This is due to the high thermal diffusivity of the underlying silicon substrate.

3.2. Temperature measurement during pulsed heating

A series of electric pulses was supplied to a submicron heater device of initial resistance, 13.6 Ω, loaded with deionized water and that was connected to the circuit sketched in Fig. 3. The pulse duration was gradually decreased when increasing the current to avoid the damage of the device. The temperature of the heater subjected to pulsed heating reaches steady state in few microseconds. A boiling phenomenon taking place on such a small heater is expected to induce a considerable temperature perturbation and thus to be electrically detected. For current supply below 24.0 mA no boiling was observed. Above 24 mA, two distinct characteristics were identified. (I) Boiling occurs after reaching pseudo-steady state meaning that boiling occurs after the heat losses equal the input power (24.2–25 mA); (II) Boiling was observed during the transient state (above 26 mA).

These two distinct characteristics obtained for water at atmospheric pressure are shown in Fig. 6. Fig. 6a shows a representative temperature evolution curve with a fast temperature increase till reaching the pseudo-steady temperature. The duration of the transient was 2 μs and the pseudo-steady temperature was 250 °C. After a few microseconds (6.4 μs in the case represented in Fig. 6a) an abrupt temperature increase is observed. This abrupt temperature increase is associated with the formation of vapor on the heater. When the vapor forms it thermally insulates the heater [9,11] therefore the average temperature of the heater increases. After this first abrupt temperature increase the temperature starts to oscillate around the pseudo-

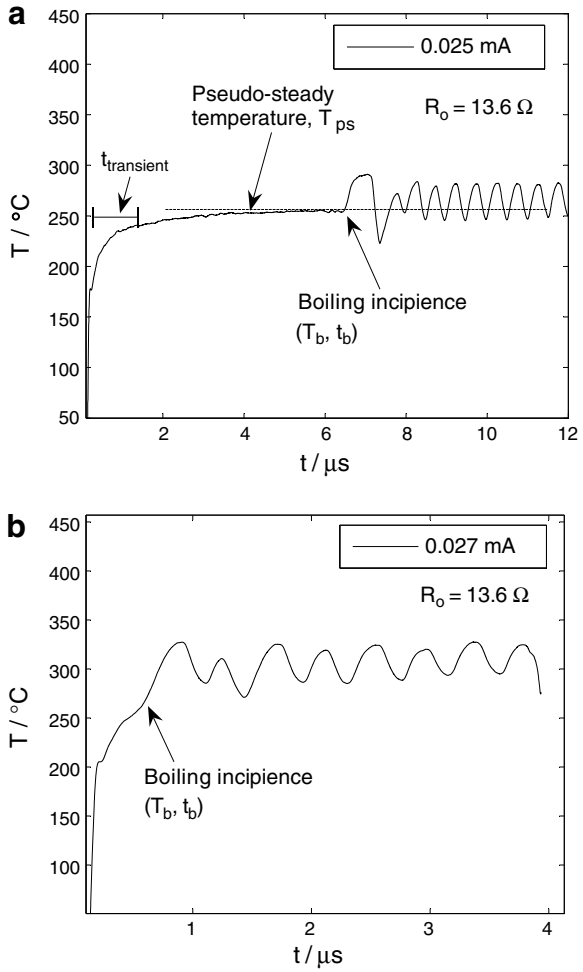

Fig. 6. (a) A representative temperature evolution curve showing the fast temperature increase till reaching the pseudo-steady temperature. The kink in the temperature evolution indicates the boiling incipience. (b) A representative temperature evolution curve for high current amplitude supply (>26 mA). The kink in the temperature evolution occurs during the transient.

steady temperature. The oscillation is maintained for approximately 40 μs (not shown entirely in the scale of Fig. 6a). More details about this oscillatory phenomenon will be provided in the following section. Increasing the current amplitude reduced the time lag of the first temperature kink with respect to the origin in a very consistent manner not affecting the pseudo-steady temperature.

Fig. 6b shows a temperature evolution curve for an experiment with higher current amplitude (>26 mA), corresponding to the category II. In this example a kink in the temperature curve can be observed already during the fast transient state. This implies that the boiling incipience occurs before reaching the pseudo-steady temperature. In the curves following this pattern the kink identifying the boiling incipience is less sharp and we used the inflection of the curve to determine the boiling incipience temperature and time. For each experiment, we define the boiling incipience temperature, the boiling incipience time and the rate of temperature rise. The boiling incipience temperature T_b is defined as the temperature at which the abrupt increase in the temperature evolution curve occurs and the boiling time t_b is defined as the time lapsed from the heating onset until this abrupt increase. The rate of temperature rise is defined as the ratio of the boiling temperature to the boiling incipience time. For the cases in which the thermal response of the heater (temperature evolution curve) features a plateau (category I) we defined the rate of temperature rise as the ratio of the pseudo-steady temperature (or temperature of the plateau), T_{ps} to the time duration of the transient. For category II, depicted in Fig. 6b, the standard definition of the rate of temperature rise mentioned above was used.

3.2.1. Effect of current intensity on boiling incipience

Fig. 7a shows the boiling incipience temperature obtained for a series of experiments. For experiments in which boiling occurs only after reaching the pseudo-steady temperature (category I), the boiling temperature does not vary significantly with the current amplitude. On the other hand, for currents above 26 mA (category II) the boiling temperature increases with the current amplitude.

Several measurements were made for the same electrical parameters (for the same heating pulse) and the thermal response curves showed that the time at which boiling initiated varied from event to event. This variation (or jittering) was of several μs in the case of 24.2 mA. Increasing the heating current had the twofold effect of shortening the boiling time and leading to less jittering in the repeated heating events. This implies that an increase in the current level makes the process more predictable. Fig. 7b depicts the measured values of boiling incipience times with the error bars signifying the jittering effect. Boiling was even observed 0.35 μs after starting the heating for 29.3 mA.

Table 1 contains values of boiling incipience temperature obtained by other authors. In the works by Deng et al. [14,16] the boiling incipience was detected by a "V-shaped" temperature change. The last row refers to the device used by Avedisian et al. [9]. The rate of temperature rise measured for this device was 2.5×10^8 K/s, which is one of the highest values obtained in pulsed heater experiments. In the present work a maximum rate of temperature rise of 8.2×10^8 K/s was reached for 29.3 mA. This very high value of the rate of temperature rise is due to the small dimensions of the heater compared with previous studies.

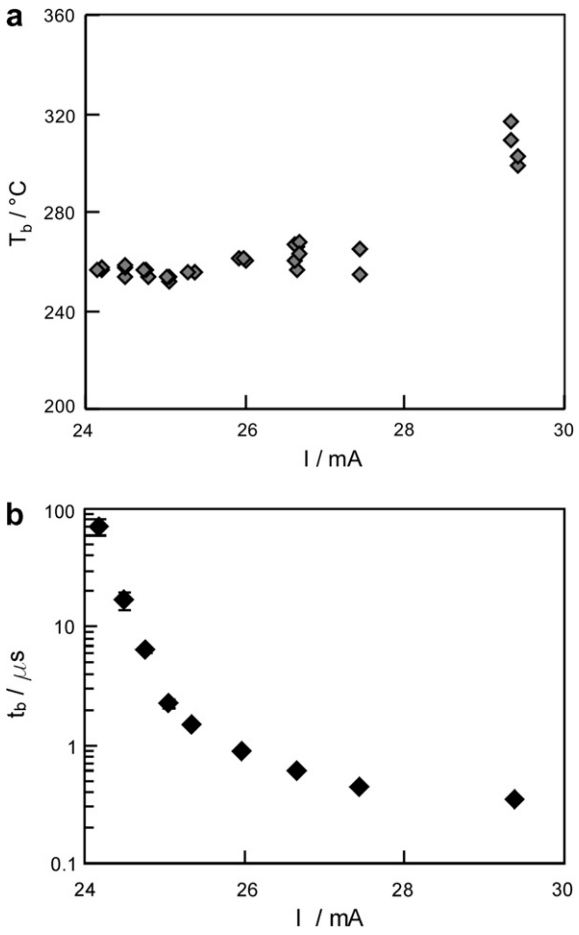

Fig. 7. (a) Boiling temperature, T_b, for different current pulses. for a heater of initial resistance 13.6 Ω. (b) Boiling time, t_b, as a function of current supply.

Table 1
Boiling incipience temperatures obtained in other works with microheaters

Feature size (μm^2)	Pulse duration (μs)	T_b (°C)	Rate of temperature rise (K/s)	t_b (μs)	Reference
0.5 × 0.5	1.66	245	16×10^6	51	[14]
1 × 0.5	1.66	207	12×10^6	60	[14]
2 × 1	1.66	214	10^6–10^7	60	[16]
65 × 65	5	283	2.5×10^8	0.7	[9]

3.3. Frequency analysis of the oscillations of the temperature evolution

In the previous section, the temperature oscillations, once initiated, were maintained until the end of the pulse.

In order to determine how long this oscillation exists, we performed a series of experiments by applying longer heating pulses to a heater of initial resistance $R_0 = 16.85\ \Omega$. The general trend is shown in Fig. 8. The temperature evolution curve is recorded for a heating pulse of 70 μs, after boiling incipience the temperature starts to oscillate at high frequency (MHz) for about 40μs. The amplitude of the oscillation decays in time and the mean temperature slowly increases.

To analyze the frequency components contained in the signal, fast Fourier transformation (FFT) was used. Since the oscillation frequency varied with time, the data points of the three regions of the signal indicated in Fig. 8 as A, B and C were analyzed separately. The result of the FFT analysis is presented in Fig. 8b. The time interval considered for the analysis is indicated at the top of each plot. There exists a distinct main frequency component in each region, which is indicated in the figure and it increases during the pulse duration from 2.68 to 3.08 and finally 3.24 MHz. In the plot corresponding to the region C there is an important contribution of lower frequencies induced by the shift of the average temperature and to the attenuation of the amplitude of the temperature oscillation. The increase of the temperature frequency with time may be due to many interconnected phenomena. For our discussion we will focus on the frequency associated with the oscillation following boiling incipience (region A).

3.3.1. Effect of the heating pulse amplitude

The influence of the heating pulse amplitude on the frequency of the temperature oscillation was assessed for a series of experiments with increasing current amplitude. The result is depicted in Fig. 9 where it can be seen that the frequency increases with current intensity in all the regions studied and particularly in the region A (immediately after boiling incipience), where the frequency increases as the current amplitude increases from 2.8 to 3.8 MHz. The boiling temperature in the cases studied

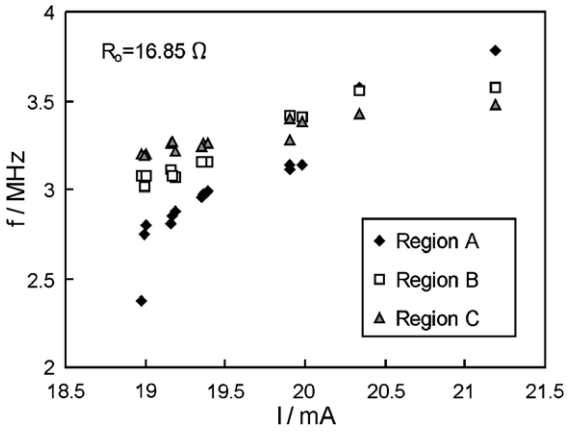

Fig. 9. Main frequency of the temperature oscillation versus current amplitude for a heater of $R_0 = 16.85\ \Omega$.

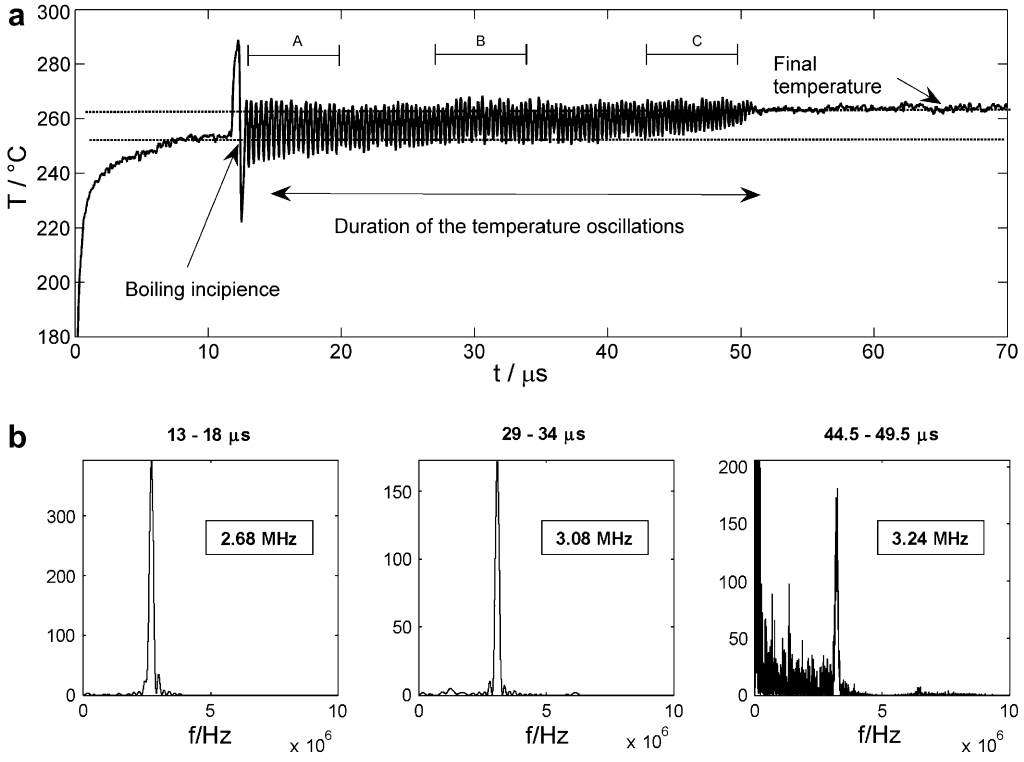

Fig. 8. Temperature evolution curve recorded for a heating pulse of 70 μs duration. After the boiling incipience (first abrupt temperature increase) the temperature starts to oscillate. The oscillation stays for about 40 μs decaying in time. (b) Fast Fourier transformation was applied to analyze the oscillation in three regions A, B and C.

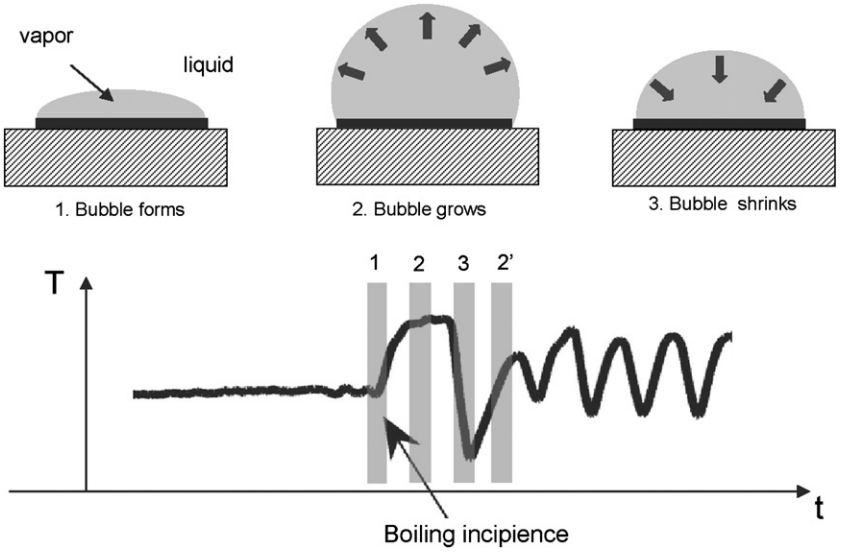

Fig. 10. Temperature scenario for bubble oscillation mechanism.

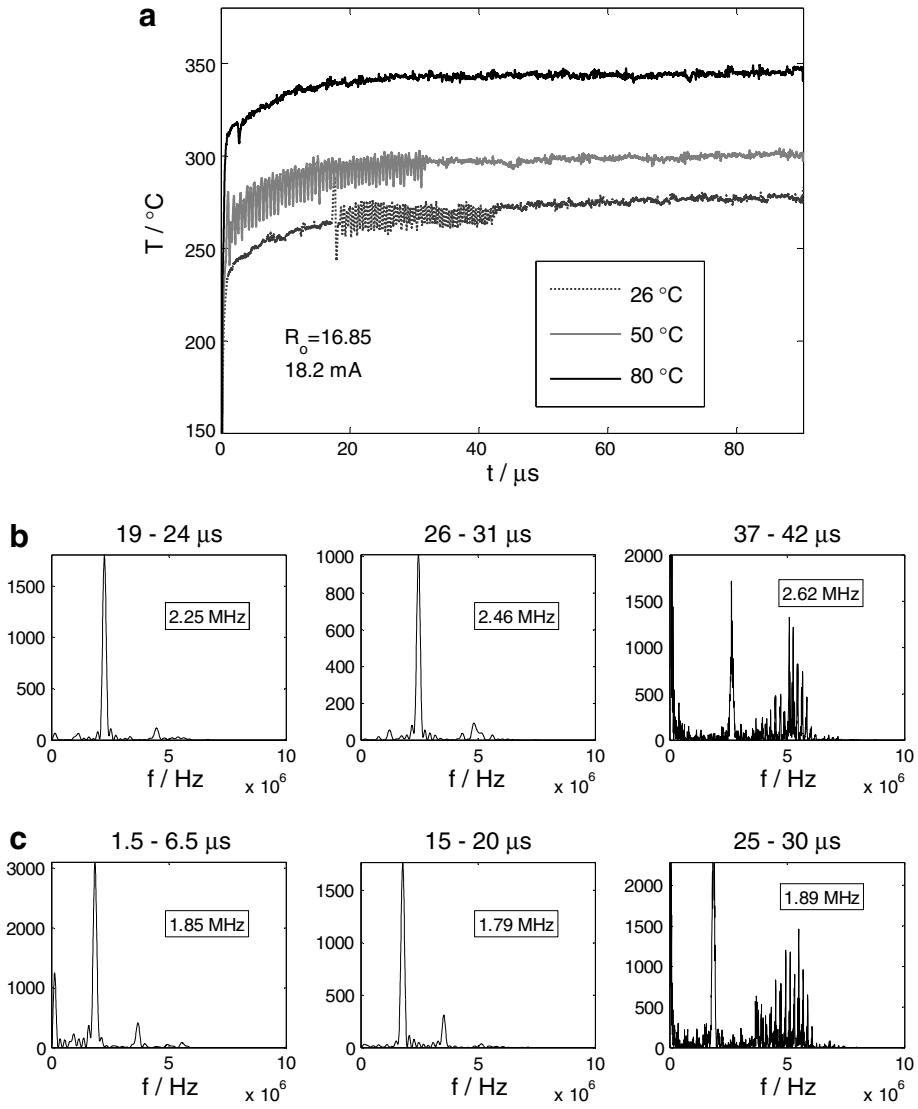

Fig. 11. (a) Temperature evolution curve for experiments performed with three different initial liquid temperatures: 26 °C (room temperature), 50 °C and 80 °C. (b) Fast Fourier transformation of the oscillation appearing after initiating boiling for liquid at room temperature (c) and for the liquid at 50 °C.

herein was 250 °C and did not vary much in the range of current amplitudes used. The temperature of the heater after the oscillation stops (the final temperature), shifted from 264 °C (for 18.9 mA) to 320 °C (for 21.2 mA).

3.3.2. Explanation of temperature oscillations

The oscillation observed in the temperature evolution curve is a boiling-induced phenomenon, directly related to the microbubble formation and decay as it can be deduced by the fact that this oscillation does not occur in the experiments performed without liquid or when the current pulse was not intense enough to induce vapor formation. A plausible explanation behind this phenomenon can be found by considering the difference between two bubble growth scenarios: (1) growth in an initially uniform superheated liquid and (2) growth in the electrically heated surface. When a vapor bubble forms in the superheated liquid, the liquid temperature gradient in radial direction around a growing bubble would have a positive slope. The heat transfer by conduction between the vapor and the liquid phase would be towards the vapor phase, providing the latent heat needed to sustain the growth of the bubble. In the second scenario (Fig. 10) the vapor covers the heated surface and energy is supplied by the surface to the bubble interface by conduction through the vapor phase. The temperature gradient in the liquid has a negative slope because the liquid away from the hot surface is colder than in the superheated vapor. Conduction heat transfer to the liquid cools down the interface. As the bubble grows and the distance between the heat supplying surface and the interface increases, the heat removal from the interface becomes larger than the heat supply to it. This will cause the bubble to

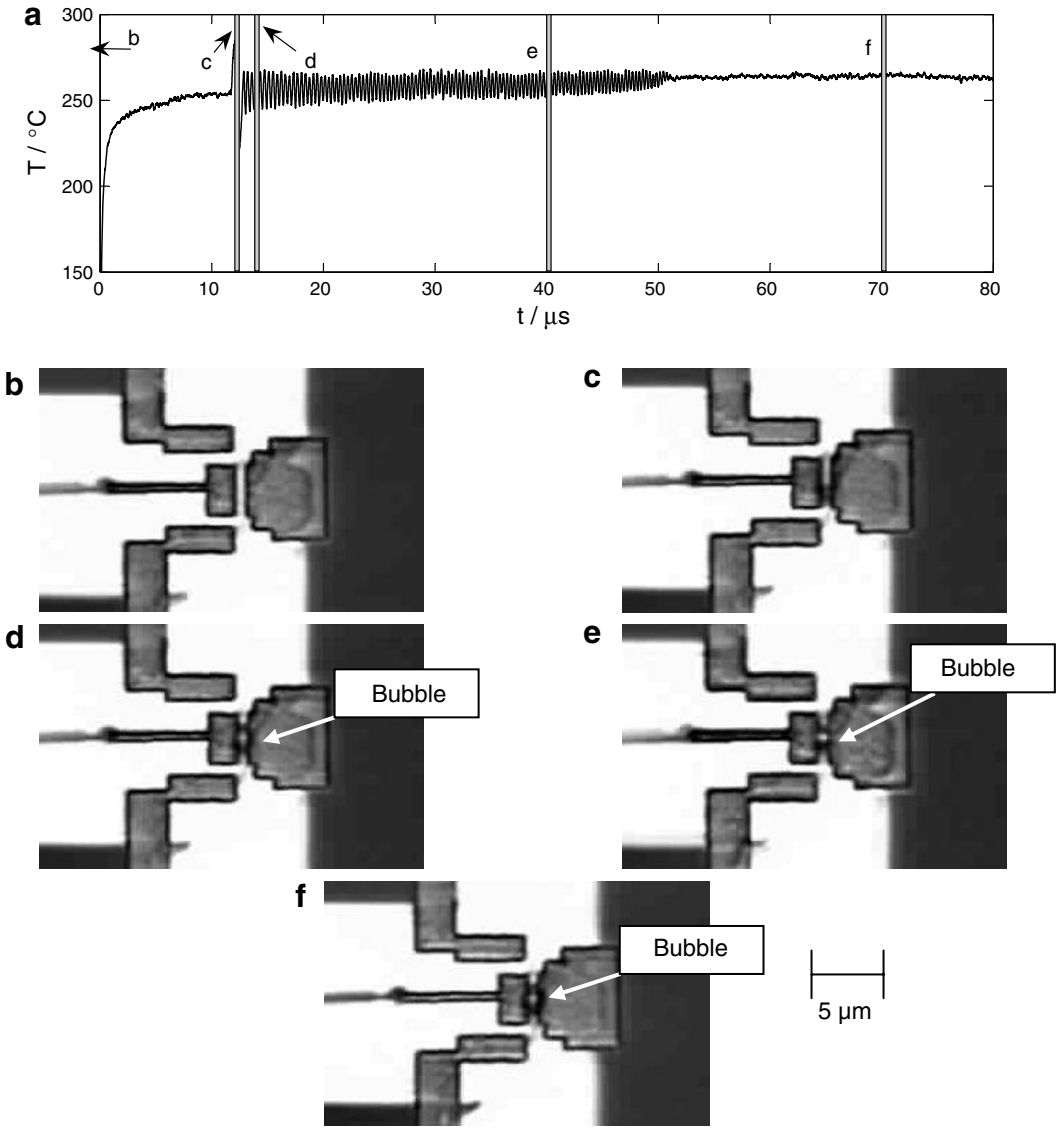

Fig. 12. (a) Temperature evolution curve showing the instants when images are acquired during visualization experiments. (b) Submicron heater before applying the heating pulse (c) Image acquired after boiling incipience. (d) Image acquired after a few temperature oscillation cycles. (e) Image acquired 40 μs after heating onset. (f) Image acquired 70 μs after heating onset.

start collapsing until the interface is close enough to the heating surface so that the heat supply to the interface is large enough to cause bubble regrowth. The phenomenon repeats itself as long as the surrounding fluid remains cold enough to provide the heat removal counteracting the heat supply to the interface, thus explaining the oscillatory behavior discussed earlier.

3.3.3. The effect of the initial temperature of the liquid

To investigate the effect of the liquid initial temperature we performed the same heating experiment with different initial liquid temperatures. Based on the proposed mechanism, the oscillation frequency should decrease, its amplitude should increase and the oscillation should disappear as the temperature of the liquid keeps increasing. To heat the liquid, the chip holder was located on an aluminum block with a drilled hole to insert a heating element. The aluminum block was fabricated to fit underneath the ceramic IC package. A dc source (TTi EX344T) supplies the necessary power to the heater element. The temperatures in the aluminum block under the carrier and in the liquid above the heater were monitored using two thermocouples (Type K). The temperature of the liquid near the heater was obtained by averaging the two thermocouple measurements. The error in determining this temperature was ± 2 °C.

A heating current of 18.6 mA was supplied to a heater of initial resistance of 16.85 Ω for three different bulk liquid temperatures: (1) 26 °C, (2) 50 °C and (3) 80 °C. The boiling incipience took place 17.19, 0.75 and 0.4 μs after initiating the electrical heating, respectively. The temperature differences between the heater and the liquid at boiling incipience are 243 °C, 210 °C and 180 °C, respectively. The temperature oscillation previously observed at room temperature (26 °C) was still present at lower frequencies at liquid temperature of 50 °C, but it was not observed when the liquid temperature was set at 80 °C Fig. 11a. For liquid at room temperature an FFT of the data after initiating boiling (19–24 μs) yields a main frequency of the oscillation at 2.25 MHz. For the liquid at 50 °C the FFT of the data in the data points following the first perturbation (1.5–6.5 μs) reveals a main frequency component of the temperature oscillation of 1.85 MHz, signifying a longer bubble growth period due to less effective cooling until collapse that is in agreement with the given mechanism.

3.4. Submicron bubble visualization

The photographs in Fig. 12 were taken during pulsed heating experiments at different instants of the process. Fig. 12a indicates the instants corresponding to the images in (b)–(f). The blur in the images is caused by the long duration of the light flash, (b) shows the heater before any heating for comparison with the images showing a bubble formed right after boiling incipience, (c), few microseconds after boiling incipience, (d), 40 microseconds after heating onset, and after several oscillation cycles (e), and the last image was taken when the oscillations stopped and it shows a bubble located on the center of the heater (f). The bubble stayed till the end of the heating pulse.

4. Conclusions

The heating and boiling phenomena triggered by a submicron thin film strip heater were investigated in this work. Short electrical pulses (5–70 μs) were used to increase the heater temperature in contact with liquid water. We measured the voltage drop across the heater and calculated the instantaneous temperature (spatially averaged) of the heater. The temperature evolution showed a very fast transient followed by a temperature plateau. If the temperature at the plateau (pseudo-steady temperature) is high enough, a sudden increase of temperature takes place after a certain time, indicating the formation of vapor on the heater. An increase of the supplied current intensity shortens the time lag between heating onset and boiling incipience and increases the boiling temperature. An interesting oscillation in the temperature curve was observed. The frequency of the oscillation is in the order of MHz and it increases with heating pulse amplitude. The physics behind this effect was explained in the context of this work. Increasing the bulk temperature of the liquid made the oscillations disappear verifying the hypothesis that the oscillations is caused by the counteracting effects of heat supply to the interface by the heater and heat removal by the cooling effect of the subcooled liquid.

The electronic detection of boiling was underpinned by visualization of the surface of the immersed heater subjected to pulse heating. Submicron scale bubbles were visualized for different times during the heating phase using a pulsed visualization system where the frame acquisition and illumination system is synchronized with the heating pulse.

Acknowledgments

The fruitful discussions with Dr. Mathias Dietzel (LTNT/ETH Zurich) are greatly appreciated. This work was supported by the Swiss National Science Foundation under Grant Number 2000-067738/1.

References

[1] J. Bartak, A study of the rapid depressurization of hot water and the dynamics of vapour bubble generation in superheated water, Int. J. Multiphase Flow 16 (1990) 789–798.
[2] M. Staples, K. Daniel, M.J. Cima, R. Langer, Application of micro- and nano-electromechanical devices to drug delivery, Pharma. Res. 23 (2006) 847–863.
[3] K.W. Oh, C.H. Ahn, A review of microvalves, J. Micromech. Microeng. 16 (2006) R13–R39.
[4] D.J. Laser, J.G. Santiago, A review of micropumps, J. Micromech. Microeng. 14 (2004) R35–R64.
[5] S. Baik, J.P. Blanchard, Development of micro-diesel injector nozzles via microelectromechanical systems technology and effects on spray

characteristics, J. Eng. Gas Turbines Power – Trans. Asme 125 (2003) 427–434.
[6] Y.K. Lee, U.C. Yi, F.G. Tseng, C.J. Kim, C.M. Ho, Fuel injection by a thermal microinjector, in: Proceedings of MEMS, ASME International Mechanical Engineering Nashville, Tennessee, USA, 1999, pp. 419–425.
[7] D.K. Maurya, S. Das, S.K. Lahiri, Silicon MEMS vaporizing liquid microthruster with internal microheater, J. Micromech. Microeng. 15 (2005) 966–970.
[8] C. Rossi, D. Briand, M. Dumonteuil, T. Camps, P.Q. Pham, N.F. de Rooij, Matrix of 10×10 addressed solid propellant microthrusters: review of the technologies, Sensors Actuat. A – Phys. 126 (2006) 241–252.
[9] C.T. Avedisian, W.S. Osborne, F.D. McLeod, C.M. Curley, Measuring bubble nucleation temperature on the surface of a rapidly heated thermal ink-jet heater immersed in a pool of water, Proc. Royal Soc. A: Math. Phys. Eng. Sci. 455 (1999) 3875–3899.
[10] K.P. Derewnicki, Experimental studies of heat transfer and vapour formation in fast transient boiling, Int. J. Heat Mass Transfer 28 (1985) 2085–2092.
[11] S. Glod, D. Poulikakos, Z. Zhao, G. Yadigaroglu, An investigation of microscale explosive vaporization of water on an ultrathin Pt wire, Int. J. Heat Mass Transfer 45 (2002) 367–379.
[12] Y. Iida, K. Okuyama, K. Sakurai, Boiling nucleation on a very small film heater subjected to extremely rapid heating, Int. J. Heat Mass Transfer 37 (1994) 2771–2780.
[13] V.P. Skripov, P.A. Pavlov, Explosive boiling of liquids and fluctuation nucleus formation, High Temp. 8 (1970) 782.
[14] P. Deng, Y.-K. Lee, P. Cheng, Characterization of an integrated self-sensing submicron bubble actuator, in: Asia-Pacific Conference of Transducers and Micro-Nano Technology (APCOT) Sapporo, Japan, 2004, pp. 310–315.
[15] P. Deng, Y.-K. Lee, P. Cheng, Scaling effects of micro bubble actuators, in: The 13th International Conference on Solid-State Sensors, Actuators and Microsystems Seoul, Korea, 2005, pp. 1267–1271.
[16] P.G. Deng, Y.K. Lee, P. Cheng, An experimental study of heater size effect on micro bubble generation, Int. J. Heat Mass Transfer 49 (2006) 2535–2544.
[17] M.F.M. Osborne, The acoustical concomitants of cavitation and boiling, produced by a hot wire. II, J. Acoust. Soc. Am. 19 (1947) 21–29.
[18] Z. Zhao, S. Glod, D. Poulikakos, Pressure and power generation during explosive vaporization on a thin-film microheater, Int. J. Heat Mass Transfer 43 (2000) 281–296.
[19] G. Romera-Guereca, J. Lichtenberg, A. Hierlemann, D. Poulikakos, B. Kang, Explosive vaporization in microenclosures, Exp. Therm. Fluid Sci. 30 (2006) 829–836.